Supporting Information

Click chemistry-based dual nanosystem for microRNA-122 detection with single-base specificity from tumour cells

Agustín Robles-Remacho*§[#1,2,3], Ismael Martos-Jamai§[1,2,3], Mavys Tabraue-Chávez[4], Araceli Aguilar-González[1,2,3], Jose A. Laz-Ruiz[1,2,3], Victoria Cano-Cortés[1,2,3], Francisco J. López-Delgado[4], Juan J. Guardia-Monteagudo[4], Salvatore Pernagallo[4], Juan J. Diaz-Mochon*[1,2,3], and Rosario M. Sanchez-Martin[1,2,3]

[1]GENYO, Centre for Genomics and Oncological Research, Pfizer/University of Granada/Andalusian Regional Government, PTS Granada, Avenida de la Ilustración, 18016, Spain

[2]Department of Medicinal and Organic Chemistry and Excellence Research Unit of Chemistry Applied to Biomedicine and the Environment, School of Pharmacy, University of Granada, Campus Cartuja s/n, 18071, Granada, Spain

[3]Instituto de Investigación Biosanitaria ibs.GRANADA, 18012 Granada, Spain

[4]DESTINA Genomica S.L, PTS Granada, Avenida de la Innovación 1, Edificio BIC, 18100, Armilla, Spain

§These authors have contributed equally

*Corresponding authors: Agustín Robles-Remacho (agustin.robles@scilifelab.se) and Juan J. Díaz-Mochón (juanjose.diaz@genyo.es)

#Current Address: Science for Life Laboratory, Department of Biochemistry and Biophysics, Stockholm University, Stockholm, Sweden.

Table of Contents

Supporting Information 1. Chemical structure of the abasic PNA probe and SMART-Nucleobases

The abasic PNA probe, (N-terminus) AcHNLys(N_3)-OO-CACCATTgluGT***GL***ACglu ACTgluCCA (C-terminus), was designed with an abasic position (***GL***) opposite to a guanine of the hsa-miR-122-5p sequence, templating the incorporation of SMART-C-Biotin. The probe is 18-mer in length and consists of neutral PNA monomers, chiral PNA monomers with a glutamic acid-like side chain at the gamma position and an azide moiety at the N-terminus [1, 2]. The azide moiety is linked via a spacer consisting of two diethylene glycol (miniPEG) units, represented as 'OO' and the probe carries chiral PNA monomers to facilitate the integration of the SMART-Nucleobases (**Figure S1**) [2]. SMART-Nucleobases are conjugated to biotin via a PEG_{12} linker and are aldehyde modified to react with the secondary amine at the abasic site (**Figure S2**).

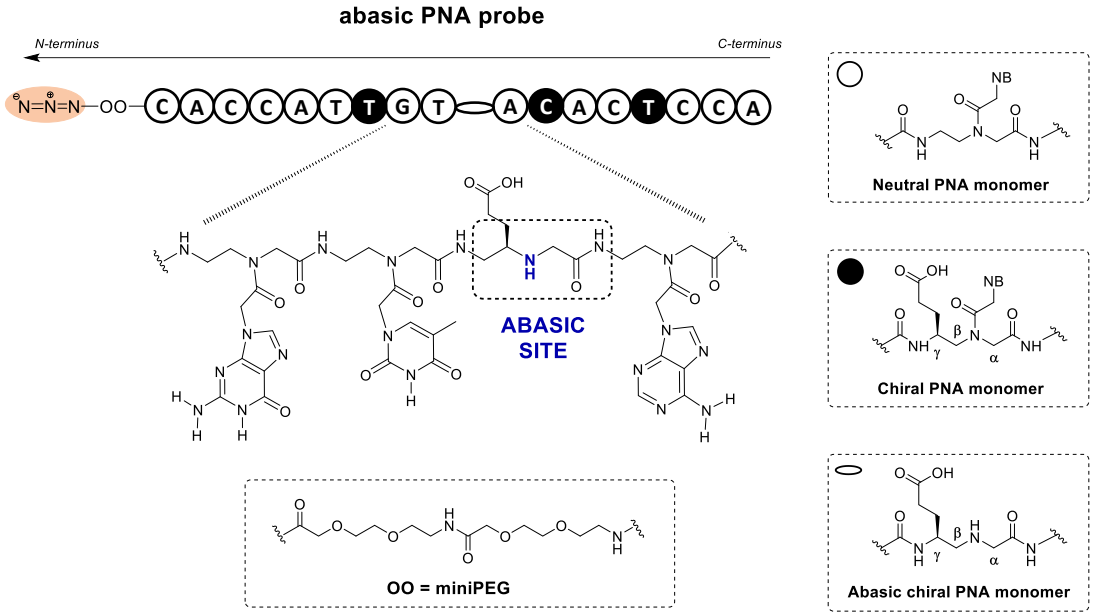

Figure S1. Chemical structure and sequence of the abasic PNA probe. The abasic site is positioned opposite a guanine nucleobase within the hsa-miR-122-5p sequence. Chiral PNA monomers facilitate the integration of the SMART-Nucleobases. The azide moiety at the N-terminus allows the click chemistry reaction with BCN-Cy5 NPs (12).

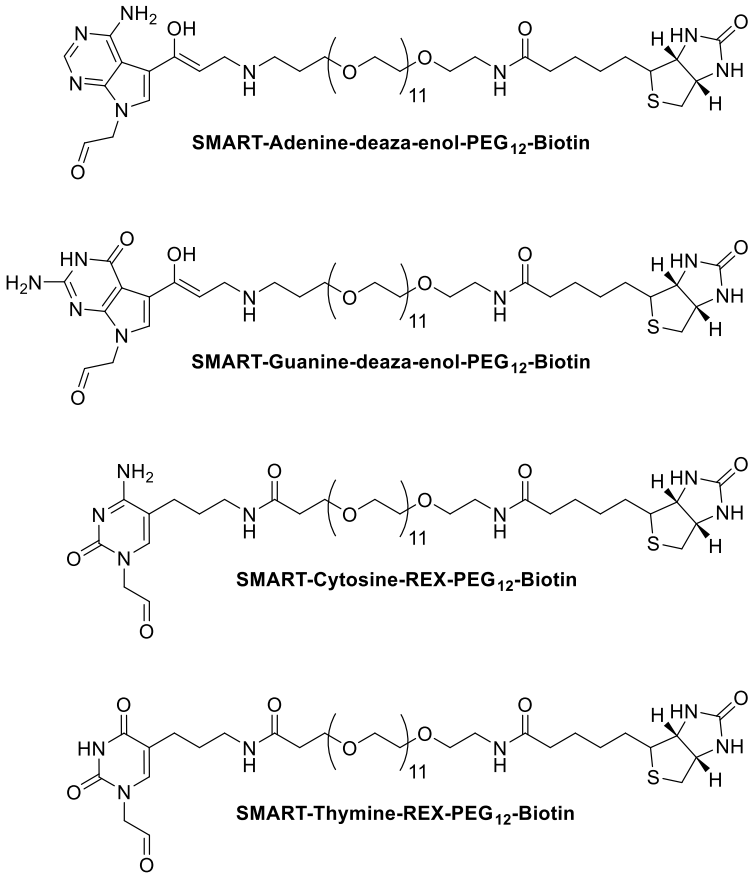

Figure S2. Chemical structure of the biotinylated SMART-Nucleobases used in the dual nanosystem.

Supporting Information 2. Oligonucleotides and abasic PNA probe sequences

Table S1. Sequences of miR-122 and miR-21 single-stranded DNA (ssDNA) and RNA (ssRNA) oligonucleotides and the abasic peptide PNA probes used in the dual nanosystem, together with the complementary SMART-Nucleobases. The nucleobases evaluated in each target sequence are underlined.

Reference miRNA	**Sequence (5'→3')**	**miRBase ID**
Hsa-miR-122-5p	UGGAGUGU**G**ACAAUGGUGUUUG	MIMAT0000421
Hsa-miR-21-5p	UAGCUUAUCA**G**AC**U**GAUGUUGA	MI0000077
ssDNA oligonucleotides	**Sequence (5'→3')**	**Complementary SMART-NB**
ssDNA-122 WT	TGGAGTGT**G**ACAATGGTGTTTG	SMART-C
ssDNA-122 SNV(T)	TGGAGTGT**T**ACAATGGTGTTTG	SMART-A
ssDNA-122 SNV(C)	TGGAGTGT**C**ACAATGGTGTTTG	SMART-G
ssDNA-122 SNV(A)	TGGAGTGT**A**ACAATGGTGTTTG	SMART-T
ssDNA-122-Cy5 WT	Cy5-TGGAGTGT**G**ACAATGGTGTTTG	SMART-C
ssDNA-21 WT	TAGCTTATCA**G**AC**T**GATGTTGA	SMART-C/A
ssRNA oligonucleotides	**Sequence (5'→3')**	**Complementary SMART-NB**
ssRNA-122 WT(G)	UGGAGUGU**G**ACAAUGGUGUUUG	SMART-C
ssRNA-122 SNV(T)	UGGAGUGU**U**ACAAUGGUGUUUG	SMART-A
ssRNA-122 SNV(C)	UGGAGUGU**C**ACAAUGGUGUUUG	SMART-G
ssRNA-122 SNV(A)	UGGAGUGU**A**ACAAUGGUGUUUG	SMART-T
Abasic PNA probes	**Sequence (N→C)**	**Abasic site**
PNA-122	Ac-Lys(N_3)-OO-*CACCAT Tglu GT**GL**A Cglu AC Tglu CCA*-NH_2	G9
PNA-21 (SA)	Ac-Lys(N_3)-OO-*CAA Cglu ATCA Gglu T**GL**T Gglu ATAAGC*-NH_2	T14
PNA-21 (SC)	Ac-Lys(N_3)-OO-*CAACA Tglu C**GL**G Tglu CTGATAAGC*-NH_2	G11

Supporting Information 3. Synthesis of PS-NPs (1), BCN-Cy5-NPs (12) and BCN-NPs (14)

3.1. Synthesis of PS-NPs (1)

3.1.1. General procedure

Aminomethyl polystyrene nanoparticles, PS-NPs (1), were prepared by dispersion polymerisation as previously described [3]. First, polyvinylpyrrolidone (PVP) (Mw 29,000, Sigma-Aldrich) was dissolved in a solution containing 86% ethanol and 14% water (final volume 10 mL) and deoxygenated with argon. At the same time, a solution of azobisisobutyronitrile (AIBN) in styrene with vinylbenzylamine hydrochloride (VBAH) and divinylbenzene (DVB) was deoxygenated and then added to the PVP/ethanol solution. The resulting mixture was stirred under argon for 1 hour and then heated to 68 °C for 15 hours. Nanoparticles were isolated by centrifugation (12,800 rpm, 15 min) and washed twice with methanol and water (10 mL each). Finally, the NPs were suspended in water (10 mL) and stored at 4 °C.

3.1.2. Solid content (SC) of the NPs emulsion (%)

A volume of PS-NP suspension (100-200 µL) was transferred to a watch glass, covered with aluminium foil and air dried at 25 °C for 15 hours. The resulting dried NPs were then weighed to determine their mass. The solid content was then calculated using the following equation:

$$SC\ (\%)\ = \frac{M}{V_s} \cdot\ 100$$

Where M = weighed mass of NPs (mg), V_s = Volume of suspension (µL).

SC of PS-NPs (**1**): 3%, 3 mg of NPs in 100 µL of solution.

3.2. Synthesis of BCN-Cy5-NPs (12)

3.2.1. General procedure

In general, coupling reactions were carried out according to solid phase peptide synthesis (SPPS) procedures as described in *Methodology 4.3. Synthesis of PS-NPs (1), BCN-Cy5-NPs (12) and BCN-NPs (14) (main text)*. This procedure resulted in bifunctionalised NPs with a cyclooctyne moiety (BCN) and a fluorophore (Cy5) (**Figure S3**).

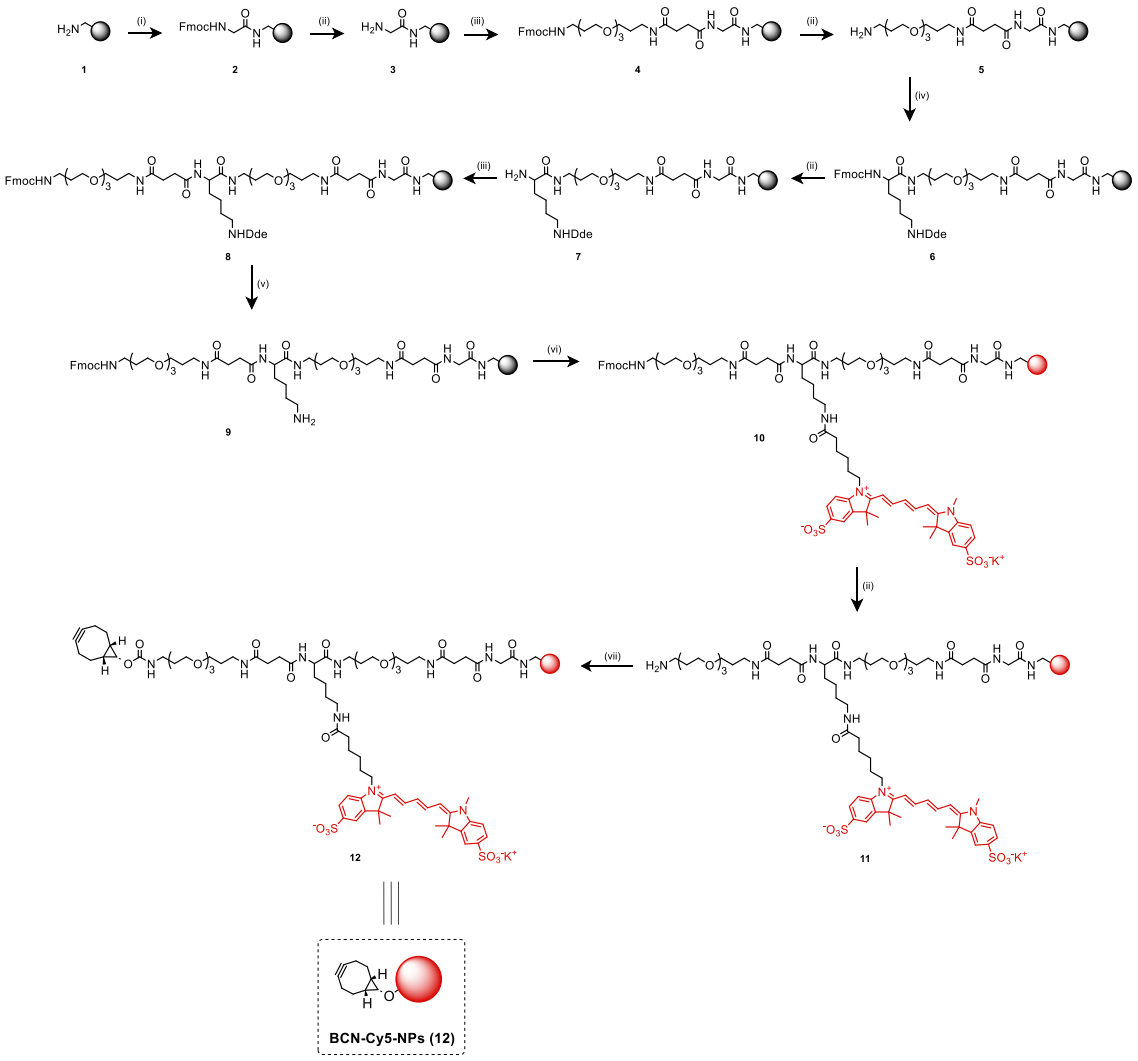

Figure S3. Synthesis of BCN-Cy5 NPs (12). A. BCN-Cy5-NPs (12) were functionalised according to standard solid phase synthesis protocols. Reagents and conditions: (i) Fmoc-Glycine-OH (50 equiv, 140 mM), Oxyma, DIC (1,400 rpm, 16 h, 25ºC); (ii) 20% piperidine in DMF (1,400 rpm, 3 × 20 min, 25ºC); (iii) Fmoc-PEG-OH (50 equiv, 140 mM), Oxyma, DIC (1,400 rpm, 16 h, 25ºC); (iv) Fmoc-Lysine(Dde)-OH (50 equiv, 140 mM), Oxyma, DIC (1,400 rpm, 16 h, 25ºC); (v) Hydroxylamine·HCl, imidazole, N-methyl-2-pyrrolidone (NMP) (1,400 rpm, 1h, 25ºC); (vi) Sulfo-Cy5 (250 µL, 0.321 µM), N,N-Diisopropylethylamine (DIPEA), anhydrous DMF (1,400 rpm, 16 h, 25ºC); (vii) BCN (20 equiv, 27.5 mM), DIPEA, anhydrous DMF (1,400 rpm, 16 h, 25ºC).

3.2.2. Quantification of load coupling through Fmoc testing

After each coupling reaction, the loading of the coupled compound on the NPs was calculated by deprotecting the Fmoc group and measuring the adduct formed. For this purpose, 1 mL of conjugated nanoparticles were resuspended in 20% piperidine in DMF for three intervals of 20 minutes each. The suspension was then centrifuged to collect the supernatants.

The three supernatants were then combined and the loading calculated using the equations:

$$Loading\left(^{mmol}/_{g}\right) = \frac{(A_{302} \cdot V)}{(\varepsilon_{302} \cdot d \cdot W)} \cdot 1000$$

$$Loading\left(^{mmol}/_{mL}\right) = Loading\left(^{mmol}/_{g}\right) \cdot SC$$

Where A_{302} = Absorbance measured at 302 nm, V = Volume of combined supernatants (mL), ε_{302} = Molar Extinction Coefficient (7800 $M^{-1}cm^{-1}$), W = Mass of NPs in mg, SC = solid content of NPs (g/mL).

3.2.3. Qualitative ninhydrin test

Each coupling reaction was monitored by qualitative ninhydrin assay as previously described [4]. Briefly, 10 µL of NPs were washed twice with methanol. Then 6 µL of reagent A (40 g phenol and 10 mL absolute ethanol) and 2 µL of reagent B (a 2 mL aliquot of an aqueous 0.65 mg/mL KCN solution diluted to 100 mL with pyridine) were added. The solution was mixed thoroughly and heated to 100 ºC for 3 minutes. The presence of primary amines is indicated by a blue colour (incomplete coupling), while their absence results in a yellow mixture (complete coupling).

3.2.4. Fmoc and Dde deprotection

Fmoc deprotection was achieved by treating Fmoc NPs with a 20% piperidine in DMF solution (1 mL, 3 × 20 min) and collecting the supernatants for loading determination. The resulting NPs were separated by centrifugation and subjected to washing steps with DMF (1 mL, × 3). Dde deprotection was performed by treating the Dde NPs with a specific Dde deprotection solution mixture consisting of 1.80 mmol NH_2OH-HCl and 1.35 mmol imidazole suspended in 5 mL NMP. This solution selectively removes the Dde group while leaving the Fmoc intact. Just before the reaction, 5 volumes of this solution were diluted with 1 volume of DMF (final volume 1 mL) and allowed to react for 1 hour at room temperature with stirring. The NPs were washed sequentially with methanol (1 mL, × 3) and DMF (1 mL, × 3) [5].

3.2.5. Quantification of nanoparticle concentration by spectrophotometric method

The concentration of NPs (NPs/µL) was determined using a spectrophotometric method as previously described [6]. The turbidity optical density of PS-NP (1) suspensions was

measured at 600 nm according to nephelometric principles. The intensity of the scattered light, which correlates with the number of NPs in the suspension, was recorded. A calibration curve was constructed using samples with known concentrations of PS-NPs (1). These curves were then fitted with a linear regression model to determine the number of NPs/µL corresponding to one unit of OD600 (**Figure S4**).

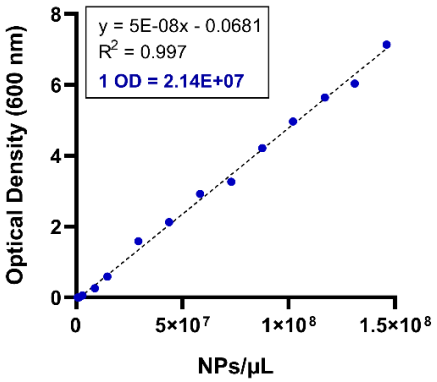

Figure S4. Calibration curve for nanoparticle concentration (OD 600 nm).

3.3. Synthesis of BCN-NPs (14)

BCN NPs (14) were synthesised following the procedure described in the previous *section 3.2* up to the preparation of Fmoc-PEG(Dde)-NPs (8). In this case, the Dde group of the lysine remained protected and the Fmoc group attached to the second PEG was removed. After Fmoc deprotection, the NPs were conjugated with BCN succinimidyl ester (20 equiv, 27.5 mM) using 0.2 µL DIPEA in 250 µL anhydrous DMF (**Figure S5**). Finally, the BCN- NPs (14) were washed and stored in water.

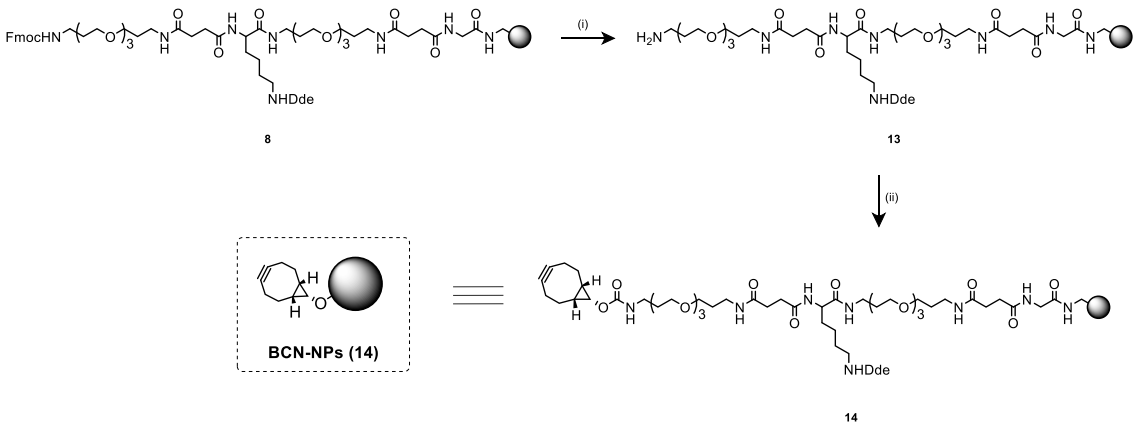

Figure S5. Synthesis of BCN-NPs (14). Reagents and conditions: (i) 20% piperidine in DMF (1,400 rpm, 3 × 20 min, 25ºC); (ii) BCN (20 equiv, 27.5 mM), DIPEA, anhydrous DMF (1,400 rpm, 16 h, 25ºC).

Supporting Information 4. Dual nanosystem characterisation

4.1. Stability of nanoparticles in different buffers

The stability of BCN-Cy5 NPs (12), BCN NPs (14) and Strep-LINARDA (3) was evaluated by dynamic light scattering (DLS) and zeta potential measurements in the different buffer solutions used (2× SSC buffer with 0.1% Tween 20, Stablitech buffer with 10% serum and Super Assay buffer). DLS analysis was used to determine the size distribution, polydispersity index (PDI) and to monitor any size changes. In addition, zeta potential was measured to assess the surface charge of the nanoparticles in these buffers, which correlates with the stability of the nanoparticle suspension (**Table S3**). A comparison between BCN-Cy5-NPs (12) and BCN-NPs (14) showed the effect of sulfo-Cy5 conjugation, resulting in an increase in size and a more negative surface charge due to the presence of sulfonic groups. Similarly, Strep-LINARDA (3) showed a negative surface charge due to the presence of carboxylic groups (**Figure S6**).

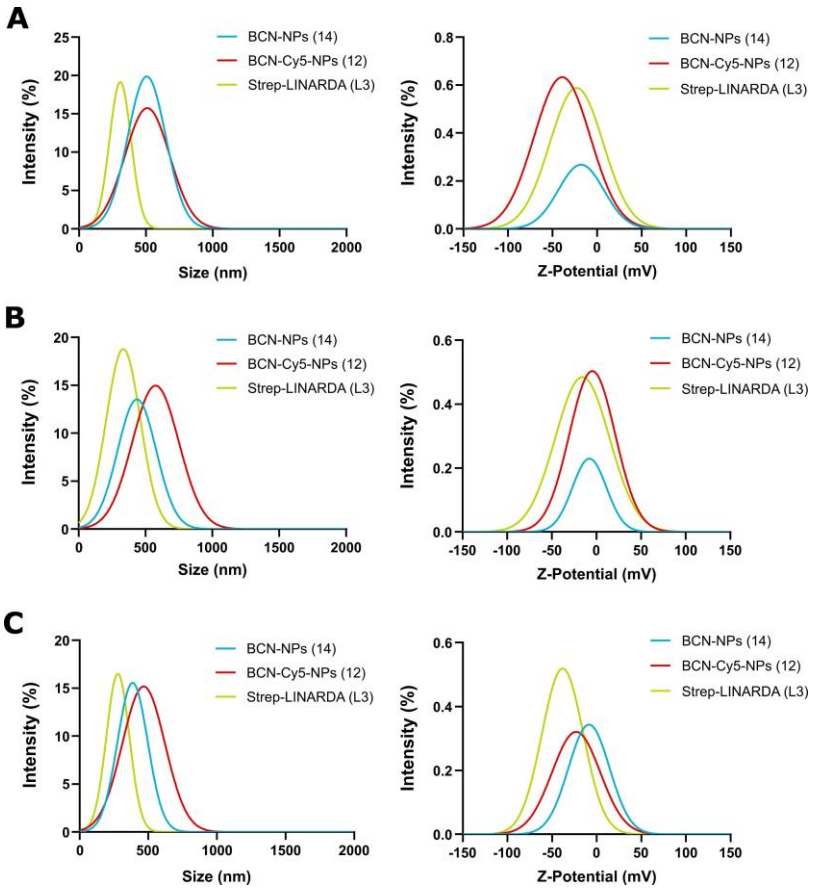

Figure S6. Size distribution measured by DLS (left) and zeta potential values (right) for BCN-Cy5-NPs (12), BCN-NPs (14) and Strep-LINARDA (L3) in SSC 2× with 0.1% Tween 20 (A), Stablitech with 10% serum (B) and Super Assay Buffer (C).

Table S3. Mean values for size, PDI and zeta potential measurements.

Nanoparticles	2× SSC with 0.1% Tween 20 buffer			Stablitech buffer with 10% serum			Super Assay buffer		
	Size (nm)	PDI	ZP (mV)	Size (nm)	PDI	ZP (mV)	Size (nm)	PDI	ZP (mV)
BCN-Cy5-NPs (12)	476.3 ± 24.2	0.333	-34.7 ± 1.5	569.4 ± 24.2	0.462	-6.7 ± 0.5	492.5 ± 22.8	0.446	-21.8 ± 3.9
BCN-NPs (14)	407.2 ± 5.3	0.197	-19.8 ± 1.6	433.8 ± 4.5	0.432	-6.3 ± 1.1	402.0 ± 9.2	0.255	-8.9 ± 1.2
Strep-LINARDA (3)	348.1 ± 21.1	0.183	-27.3 ± 0.4	335.8 ± 29.4	0.470	-9.8 ± 0.9	334.9 ± 25.5	0.360	-32.9 ± 7.4

4.2. Detection of ssRNA-122

We evaluated the detection of ssRNA-122, which represents the mature sequence of hsa-miR-122: UGGAGAGUGUGACAAUGGUGUUUG (ID MIMAT0000421). To test the specificity for ssRNA-122 detection, we performed three reactions: first, a simple mixture of both nanoparticles; second, with all components present except the PNA probe; and third, with all components present and including ssRNA-122. The reaction was performed according to the methodology described in the main text. Analysis by FACSVerse (n=3) showed positive signals only in the third case, demonstrating the specific and effective detection of ssRNA-122.

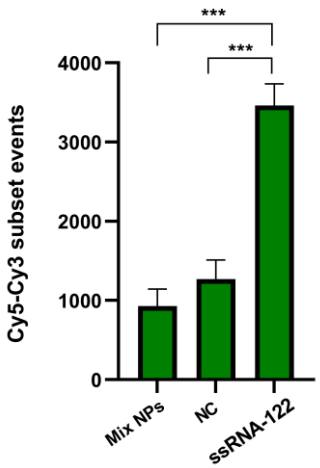

Figure S7. Detection of ssRNA-122 using the dual nanosystem. The number of events was recorded detecting both nanoparticles mixed in solution (Mix NPs), when all the components were present but without ssDNA-122, as negative control (NC) and when ssDNA-122 was present, detecting a significant increase of Cy5+/Cy3+ signal (Dual NS). Data were analysed using a non-parametric t-test (n=3).

4.3. DiagNano™ as detection nanoparticles

To further evaluate the dual nanosystem and explore commercial alternatives to Strep-LINARDA (3), we investigated additional silica nanoparticles. We evaluated DiagNano™ (DNG-L270) from CD Bioparticles (USA), 500 nm Cy3-labelled silica nanoparticles coated with streptavidin. The DCL reaction was performed under the same conditions as described in *section 2.6 (main text)* and, following the click chemistry reaction with BCN-Cy5 NPs (12), we added DiagNano™ at a concentration of 25,000 NPs/µL in Super Assay buffer and incubated at 30 °C for 30 min. The sample was then analysed by FACSVerse in a final volume of 200 µL (**Figure S7**). The result demonstrated the versatility of the dual nanosystem by successfully detecting miR-122 when using DiagNano™.

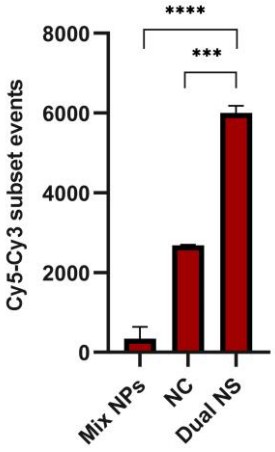

Figure S8. Dual nanosystem using DiagNano™ as recognition NPs. The number of events was recorded detecting both nanoparticles mixed in solution (Mix NPs), when all the components were present but without ssDNA-122, as negative control (NC) and when ssDNA-122 was present, detecting a significant increase of Cy5+/Cy3+ signal (Dual NS).

4.4. Detection of miR-21

We evaluated the broader applicability of the dual nanosystem by testing two additional abasic PNA probes targeting miR-21. Two nucleobase positions were analysed in synthetic ssDNA-21 sequences (5'TAGCTTATCA**G**AC**T**GATGTTGA3'). We used two abasic PNA probes, carrying the abasic site opposite a guanine and a thymine, to template the incorporation of SMART-C biotin and SMART-A biotin. The result showed that the dual nanosystem specifically detected both nucleobases (**Figure S8**).

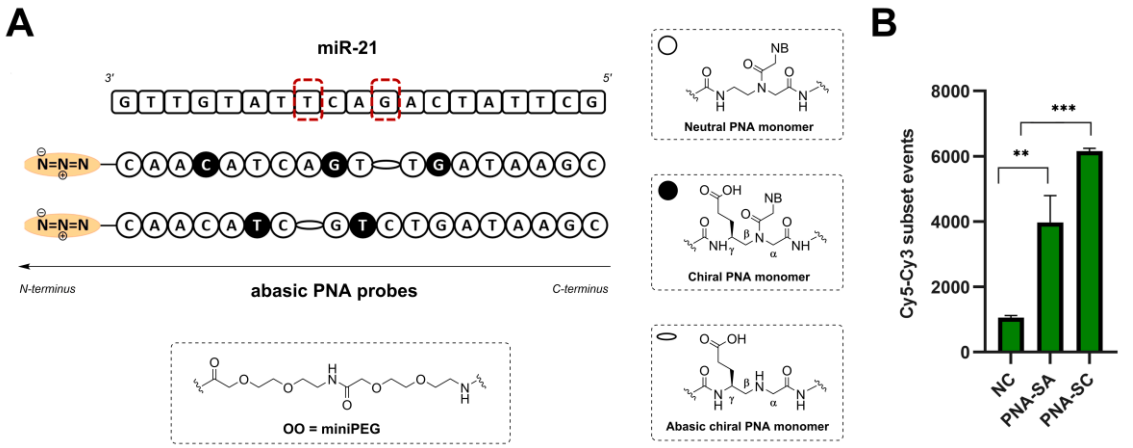

Figure S9. Detection of miR-21. A. Chemical structure and sequence of the abasic PNA probes for miR-21 detection. B. FACSVerse analysis of the number of events recorded in the negative control without ssDNA-21 (NC) and in the positive controls with the abasic PNA probe incorporating a SMART-A-Biotin (PNA-SA) and the abasic PNA probe incorporating a SMART-C-Biotin (PNA-SC).

Supporting Information 5. MALDI-TOF analysis

5.1. Evaluation of SMART-T-Biotin specificity

An additional assay was performed to confirm the detection of SMART-T-Biotin due to its similar mass to SMART-C-Biotin. Three DCL reactions were performed using ssDNA-122 SNV(A) and a mixture containing all four SMART nucleobases, but, only the concentration of SMART-T-Biotin was systematically increased (×1, ×2, ×5). In the spectra, we observed a proportional increase in signal (**Figure S9**), confirming that this signal is specific to ST-Biotin. The data obtained from the spectra for each main peak and the relative percentage of incorporation are shown in **Table S3**.

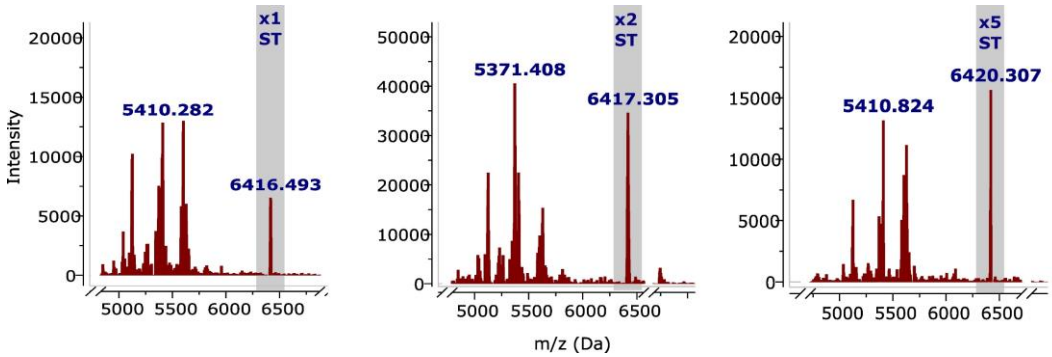

Figure S10. MALDI-TOF analysis of ssDNA-122 SNV(A). Three DCL reactions were performed with a mixture containing the four SMART nucleobases was used, with the concentration of ST-biotin systematically increased (×1, ×2, ×5). A proportional increase in signal was observed in the spectra, confirming the specificity of ST-biotin.

5.2. Analysis of SNVs in ssRNA-122

To further test the specificity and cross-reactivity of the biotinylated SMART-Nucleobases using ssRNA-122 as template instead of ssDNA-122, we performed a MALDI-TOF analysis following the procedure described in the *section 2.8. (main manuscript).* The templates used were four ssRNA-122 sequences that differ only in one nucleotide (5'UGGAGUGU-**G/A/C/U**-ACAAUGGUGUUUG3'). The spectra showed that only the complementary biotinylated SMART-Nucleobase can react, demonstrating the versatility of the method to analyse both DNA and RNA templates and its ability to discriminate between SNVs (**Figure S10**). The data obtained from the spectra for each main peak and the relative percentage of incorporation are shown in **Table S4**. In addition, the data obtained from the spectrum for the analysis of ssDNA-122 shown in the *section 2.3 (main text)* are presented in **Table S3**.

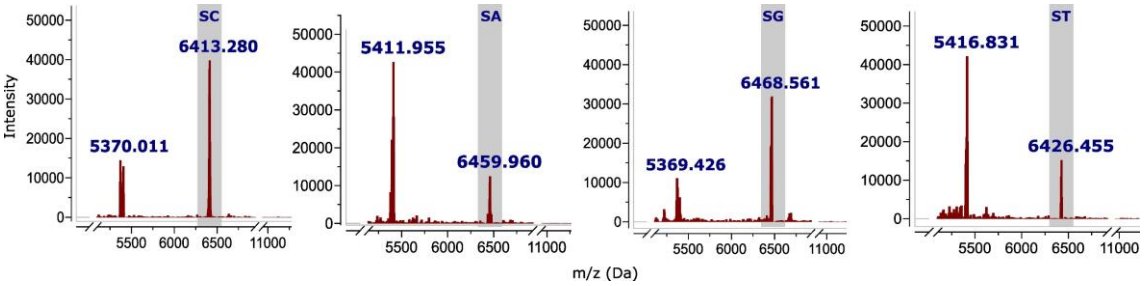

Figure S11. MALDI-TOF analysis of ssRNA-122 for SNV detection and assessment of cross-reactivity between SMART-Nucleobases. Mass differences between the two peaks provide the molecular mass of the incorporated SMART nucleobase. In the spectra of SMART-A-Biotin (SA) and SMART-T-Biotin (ST), the peak attributed to the unreacted abasic PNA probe corresponds to potassium adducts [M+K]+.

Table S3. MALDI-TOF spectra data were used to evaluate the specificity of SMART-T-Biotin and the SNV evaluation of ssRNA-122 and ssDNA-122. Analyses were performed in duplicate with four readings on the instrument. Results are presented as mean ± standard deviation.

ST-Biotin concentration	**N_3-DGL-122 peak (m/z)**	**N_3-DGL-122 + ST-Biotin peak (m/z)***	**Mean ST-Biotin incorporation (%)**
1 ×	5371.8 ± 1.3	6412.8 ± 3.6	12.8 ± 6.8
2 ×	5369.3 ± 3.3	6412.5 ± 6.9	22.0 ± 9.6
5 ×	5367.8 ± 2.2	6413.0 ± 4.7	24.8 ± 3.0
NC	5368.0 ± 1.0	-	-
ssRNA-122 SNVs	**N_3-DGL-122 peak (m/z)**	**N_3-DGL-122 + SMART-NB peak (m/z)***	**Mean SMART-NB incorporation (%)**
ssRNA-122 WT(G)	5404.3 ± 8.4	6414.3 ± 8.8	76.3 ± 2.6
ssRNA-122 SNV(T)	5388.0 ± 5.5	6451.5 ± 9.3	17.8 ± 2.1
ssRNA-122 SNV(C)	5389.3 ± 5.7	6464.8 ± 8.7	72.8 ± 8.8
ssRNA-122 SNV(A)	5404.0 ± 7.9	6413.0 ± 9.3	18.0 ± 4.5
NC	5394.5 ± 1.0	-	-
ssDNA-122 SNVs	**N_3-DGL-122 peak (m/z)**	**N_3-DGL-122 + SMART-NB peak (m/z)***	**Mean SMART-NB incorporation (%)**
ssDNA-122 WT(G)	5369.8 ± 4.0	6409.8 ± 5.0	31.8 ± 8.3
ssDNA-122 SNV(T)	5367.5 ± 2.5	6444.0 ± 5.5	22.0 ± 5.7
ssDNA-122 SNV(C)	5366.8 ± 5.0	6457.5 ± 4.8	25.8 ± 4.8
ssDNA-122 SNV(A)	5373.0 ± 2.4	6412.8 ± 5.0	6.0 ± 1.8
NC	5379.0 ± 11.3	-	-

References

[1] F.R. Bowler, J.J. Diaz-Mochon, M.D. Swift, M. Bradley, DNA analysis by dynamic chemistry, Angew. Chemie - Int. Ed. 49 (2010) 1809–1812. https://doi.org/10.1002/anie.200905699.

[2] H.A. Ilyine, J.J. Diaz-Mochon, S. Pernagallo, M.T. Chavez, M.A. Fara, PNA Probe, WO 2018/011320 A1, 2018.

[3] A. Unciti-Broceta, E.M. V Johansson, R.M. Yusop, R.M. Sánchez-Martín, M. Bradley, Synthesis of polystyrene microspheres and functionalization with Pd^0 nanoparticles to perform bioorthogonal organometallic chemistry in living cells, Nat Protoc 7 (2012) 1207–1218. https://doi.org/10.1038/nprot.2012.052.

[4] V.K. Sarin, S.B.H. Kent, J.P. Tam, R.B. Merrifield, Quantitative monitoring of solid-phase peptide synthesis by the ninhydrin reaction, Anal Biochem 117 (1981) 147–157. https://doi.org/10.1016/0003-2697(81)90704-1.

[5] J.J. Díaz-Mochón, L. Bialy, M. Bradley, Full Orthogonality between Dde and Fmoc: The Direct Synthesis of PNA−Peptide Conjugates, Org Lett 6 (2004) 1127–1129. https://doi.org/10.1021/ol049905y.

[6] J.D. Unciti-Broceta, V. Cano-Cortés, P. Altea-Manzano, S. Pernagallo, J.J. Díaz-Mochón, R.M. Sánchez-Martín, Number of Nanoparticles per Cell through a Spectrophotometric Method - A key parameter to Assess Nanoparticle-based Cellular Assays, Sci Rep 5 (2015) 10091. https://doi.org/10.1038/srep10091.